# A Numerical Approach to the Optimal Control and Efficiency of the Copepod Swimmer

Bernard Bonnard, Monique Chyba, Jeremy Rouot, Daisuke Takagi

# A Numerical Approach to the Optimal Control and Efficiency of the Copepod Swimmer

B.Bonnard and M.Chyba and J.Rouot and D.Takagi

***Abstract*— The objective of this article is to make a geometric and numerical analysis about the optimal displacements of a larval copepod swimming at low Reynolds number. A simplified model of locomotion is analyzed in the framework of Sub-Riemannian geometry. In particular, the role of both normal and abnormal geodesics is related to observed geometric motions in relation with the mechanical power dissipated by the swimmer. Numerical simulations of the normal strokes illustrate the computations and the optimal strategy is presented.**

## I. INTRODUCTION

Swimming microorganisms employ a variety of mechanisms of propulsion, and they have inspired numerous models starting with undulating sheets and filaments introduced in the fifties [12], [20]. Different types of strokes are observed depending upon the circumstances which can be used to design micro-robots in relation with the purpose.
Recent studies have explored optimal strategies for swimming with minimal amount of mechanical work, an important criterion for assessing the fitness of different organisms and for designing efficient robotic swimmers [14]. Previous studies have computed optimal solutions in the framework of variational analysis or optimal control [2], [4], [5], [9], [19].

Recently a new model was developed to mimic the locomotion of larval copepods, an abundant type of zooplankton thriving in the ocean [16], [18]. The simplest form of the model, hereafter referred to as the copepod swimmer, is a symmetric body consisting of two pairs of legs, with the first pair making an angle $\theta_1$ and the second pair making an angle $\theta_2$ with respect to the displacement direction $Ox$.
The swimming velocity at $x_0$ is given by, see [18],

$$\dot{x}_0 = \frac{\dot{\theta}_1 \sin\theta_1 + \dot{\theta}_2 \sin\theta_2}{2 + \sin^2\theta_1 + \sin^2\theta_2} \tag{1}$$

and the controls are the angular velocities

$$\dot{\theta}_1 = u_1, \quad \dot{\theta}_2 = u_2. \tag{2}$$

We also have the *state constraints* $\theta_i \in [0, \pi], i = 1, 2$, and $\theta_1 \leq \theta_2$.

J. Rouot is supported by the French Space Agency CNES, R&T action R-S13/BS-005-012 and by the région Provence-Alpes-Côte d'Azur

M. Chyba and D. Takagi: 2565 McCarthy the Mall, Department of Mathematics, University of Hawaii, Honolulu, HI 96822, USA chyba@hawaii.edu, dtakagi@hawaii.edu

Bernard Bonnard and Jeremy Rouot: Inria Sophia Antipolis and Institut de Mathématiques de Bourgogne, 9 avenue Savary, 21078 Dijon, France bernard.bonnard@u-bourgogne.fr, jeremy.rouot@inria.fr

A simplified cost neglecting the fluid interaction can be identified as

$$\int_0^T (u_1^2 + u_2^2) dt \tag{3}$$

but the true cost corresponding to the mechanical energy of the system is given by the quadratic form $\dot{q}^t M \dot{q}$ where

$$M = \begin{pmatrix} 2 - \frac{1}{2}(\cos^2\theta_1 + \cos^2\theta_2) & -\frac{1}{2}\sin\theta_1 & -\frac{1}{2}\sin\theta_2 \\ -\frac{1}{2}\sin\theta_1 & \frac{1}{3} & 0 \\ -\frac{1}{2}\sin\theta_2 & 0 & \frac{1}{3} \end{pmatrix}$$

with $q = (x_0, \theta_1, \theta_2)$.
Using (1), this amounts to minimize the quadratic cost

$$\int_0^T a(q)u_1^2 + 2b(q)u_1u_2 + c(q)u_2^2 \mathrm{d}t \tag{4}$$

with

$$\begin{aligned} a &= \frac{1}{3} - \frac{\sin^2\theta_1}{2(2+\sin^2\theta_1+\sin^2\theta_2)}, \\ b &= -\frac{\sin\theta_1 \sin\theta_2}{2(2+\sin^2\theta_1+\sin^2\theta_2)}, \\ c &= \frac{1}{3} - \frac{\sin^2\theta_2}{2(2+\sin^2\theta_1+\sin^2\theta_2)}. \end{aligned}$$

This copepod swimmer serves as a suitable model for computing optimal controls in the framework of SR-geometry. The system is three-dimensional (two shape variables and one displacement variable), which is arguably simpler than the five-dimensional system (two shape variables and three displacement variables) of the previously studied Purcell swimmer where moreover the expression of the control fields are complicated see [15]. It is a global model of SR-geometry which can be analyzed in detail, showing in particular the role of normal and abnormal geodesics in the motion. In addition, the optimal controls could be compared with observations of copepods to determine whether they are optimizing their strokes to minimize energy. Copepods must swim in order to find food and escape from predators, and they have had a chance to adapt and evolve over millions of years, but it remains unknown to what extent they have adapted their strokes to maximize their swimming efficiency. Thus the model optimization could offer new insight into biological behaviour.

This article is organized into two sections. In section II, we recall some properties of the copepod swimmer [18] and the mathematical tools from geometric optimal control (see [7] for a general reference). Section III contains the contribution of this article based on a geometric analysis and numerical simulations to describe the normal strokes

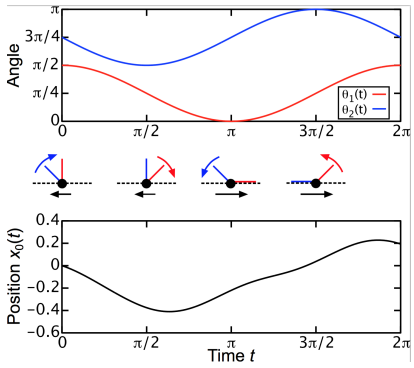


Fig. 1. Two legs oscillating sinusoidally according to $\theta_1 = \pi/4 + a\cos t$ and $\theta_2 = 3\pi/4 + a\cos(t+\pi/2)$, where $a = \pi/4$ is the amplitude. The second leg (blue) oscillates about $\Phi_2 = 3\pi/4$, while the first leg (red) oscillates about $\Phi_1 = \pi/4$ with a phase lag of $\pi/2$. The swimmer position $x_0$ translates about a fifth of the leg length after one cycle.

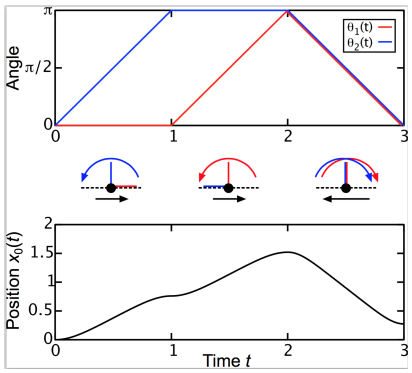


Fig. 2. Two legs paddling in sequence. The legs perform power strokes in sequence and then a recovery stroke in unison, each stroke sweeping an angle $\pi$.

in relation with the classification of periodic planar curves [3]. Finally, the optimal strokes satisfying the constraints are numerically computed using the two softwares: `Bocop` (`www.bocop.org`, [6]) and `HamPath` (`http://cots.perso.enseeiht.fr/hampath/`, [10]).

## II. Preliminary results

### A. Geometric analysis of a copepod swimmer

A (general) stroke of period $T$ consists in a periodic motion in the shape variables $(\theta_1, \theta_2)$. Assuming $x_0(0) = 0$, the corresponding displacement is $x_0(T)$. In [18], two types of geometric motions are described:

First case (Fig.1): The two legs are assumed to oscillate sinusoidally with period $2\pi$ according to

$$\theta_1 = \Phi_1 + a\cos(t), \quad \theta_2 = \Phi_2 + a\cos(t + k_2)$$

with $a = \pi/4$, $\Phi_1 = \pi/4$, $\Phi_2 = 3\pi/4$ and $k_2 = \pi/2$. This produces a displacement $x_0(2\pi) = 0.2$. Parameters $a, \Phi_1, \Phi_2$ and $k$ are designed to maximize the efficiency.

Second case (Fig.2): The two legs are paddling in sequence followed by a recovery stroke performed in unison. In this case the controls $u_1 = \dot\theta_1$, $u_2 = \dot\theta_2$ produce bang arcs to steer the angles from the boundary 0 of the domain to the boundary $\pi$, while the unison sequence corresponds to a displacement from $\pi$ to 0 with the constraint $\theta_1 = \theta_2$.

Our main objective is to relate these policies to geometric optimal control.

### B. Abnormal curves in the copepod swimmer

With $q = (x_0, \theta_1, \theta_2)$, the system is written as a driftless affine control system

$$\dot q(t) = \sum_{i=1}^{2} u_i(t) F_i(q(t))$$

where the control vector fields are given by

$$F_i = \frac{\sin\theta_i}{\Delta}\frac{\partial}{\partial x_0} + \frac{\partial}{\partial \theta_i}$$

with $\Delta = 2 + \sin^2\theta_1 + \sin^2\theta_2$. We denote by $D$ the distribution generated by the two vector fields: $D = \mathrm{span}\{F_1, F_2\}$.

The Lie bracket of two vector fields $F, G$ is computed with the convention

$$[F,G](q) = \frac{\partial F}{\partial q}(q)G(q) - \frac{\partial G}{\partial q}(q)F(q).$$

Finally, we denote by $p = (p_1, p_2, p_3)$ the adjoint vector associated with $q$.

We first recall basic facts concerning the local classification of two-dimensional distributions, in relation with abnormal curves.

*1) Local classification of two-dimensional distributions in dimension three and abnormal curves:*
Let $D = \mathrm{span}\{G_1, G_2\}$ be the distribution generated by two vectors fields $G_1, G_2$ in $\mathbb{R}^3$. Let $z = (q, p)$ and denote $H_i(z) = \langle p, G_i(q)\rangle$, $i = 1, 2$ the Hamiltonian lifts. The Poisson bracket is given by

$$\{H_1, H_2\}(z) = dH_1(\vec H_2)(z) = \langle p, [G_1, G_2](q)\rangle.$$

Abnormal curves are defined by

$$H_1(z) = H_2(z) = 0,$$

and differentiating using the dynamics

$$\frac{\mathrm{d}z}{dt} = \sum_{i=1}^{2} u_i \vec H_i(z)$$

we obtain the relations

$$\{H_1, H_2\}(z) = 0$$
$$u_1 \{\{H_1, H_2\}, H_1\}(z) + u_2 \{\{H_1, H_2\}, H_2\}(z) = 0$$

defining the corresponding abnormal controls.

Tools from singularity theory can be used to classify the distributions, see [21]. Here we present only the two (stable) models related to our study.

**Contact case.** We say that $q_0$ is a *contact point* if $\{G_1, G_2, [G_1, G_2]\}$ is of dimension three at $q_0$. At a contact point, identified to 0, there exists a system of local coordinates $q = (x, y, z)$ such that

$$D = \ker(\alpha), \qquad \alpha = y\mathrm{d}x + \mathrm{d}z.$$

Observe that $\mathrm{d}\alpha = \mathrm{d}y \wedge \mathrm{d}x$ (Darboux form) and that $\frac{\partial}{\partial z}$ is the characteristic direction of $\mathrm{d}\alpha$. This form is equivalent to

$$D = \ker(\alpha'), \qquad \alpha' = \mathrm{d}z + (x\mathrm{d}y - y\mathrm{d}x).$$

with

$$\begin{aligned} D &= \mathrm{span}\{G_1, G_2\}, \qquad & G_1 &= \frac{\partial}{\partial x} + y\frac{\partial}{\partial z}, \\ G_2 &= \frac{\partial}{\partial y} - x\frac{\partial}{\partial z}, & G_3 &= [G_1, G_2] = 2\frac{\partial}{\partial z}. \end{aligned} \tag{5}$$

**The Martinet case.** A point $q_0$ is a *Martinet point* if at $q_0$, $[G_1, G_2] \in \mathrm{span}\{G_1, G_2\}$ and at least one Lie bracket $[[G_1, G_2], G_1]$ or $[[G_1, G_2], G_2]$ does not belong to $D$. Then, there exist local coordinates $q = (x, y, z)$ near $q_0$ identified to 0 such that

$$D = \ker \omega, \qquad \omega = \mathrm{d}z - \frac{y^2}{2}\mathrm{d}x$$

where

$$\begin{aligned} &G_1 = \frac{\partial}{\partial x} + \frac{y^2}{2}\frac{\partial}{\partial z}, \quad G_2 = \frac{\partial}{\partial y}, \quad G_3 = [G_1, G_2] = y\frac{\partial}{\partial z}, \\ &[[G_1, G_2], G_1] = 0, \quad [[G_1, G_2], G_2] = \frac{\partial}{\partial z}. \end{aligned} \tag{6}$$

The surface $\Sigma : y = 0$ where $G_1, G_2, [G_1, G_2]$ are collinear is called the *Martinet surface* and is foliated by abnormal curves, solutions of $\frac{\partial}{\partial x}$. In particular, through the origin it corresponds to the curve $t \to (t, 0, 0)$.

*2) Computations in the copepod case:*
We have

$$F_3 = [F_1, F_2] = f(\theta_1, \theta_2)\frac{\partial}{\partial x_0}$$

with

$$\begin{aligned} f(\theta_1, \theta_2) &= \frac{2\sin\theta_1 \sin\theta_2(\cos\theta_1 - \cos\theta_2)}{\Delta^2}, \\ [[F_1, F_2], F_1] &= \frac{\partial f}{\partial \theta_1}(\theta_1, \theta_2)\frac{\partial}{\partial x_0}, \\ [[F_1, F_2], F_2] &= \frac{\partial f}{\partial \theta_2}(\theta_1, \theta_2)\frac{\partial}{\partial x_0}. \end{aligned}$$

We deduce the following lemma.

*Lemma 1:* The singular set $\Sigma : \{q;\ \det(F_1(q), F_2(q), [F_1, F_2](q)) = 0\}$, where the vector fields $F_1, F_2, [F_1, F_2]$ are collinear, is given by $2\sin\theta_1 \sin\theta_2(\cos\theta_1 - \cos\theta_2) = 0$ which corresponds to

- $\theta_1 = 0$ or $\pi$,
- $\theta_2 = 0$ or $\pi$,
- $\theta_1 = \theta_2$.

It is formed by the boundary of the physical domain: $\theta_i \in [0, \pi], \theta_1 \leq \theta_2$, with respective controls $u_1 = 0$, $u_2 = 0$ or $u_1 = u_2$.

*Remark 1:* The previous lemma provides the interpretation of the policy represented in Fig.2. In the shape space $(\theta_1, \theta_2)$ it corresponds to a *triangle*. The edges of the triangle are abnormal curves (where by definition the linearized system is not controllable).

*Remark 2:* A recent contribution [13] proves that a trajectory with a corner of this type cannot be optimal. (Not taking into account the state constraints)

To analyse the first situation of Fig.1, the mechanical energy has to be used in relation with SR-geometry.

### C. Sub-Riemannian geometry

The problem is written

$$\dot{q} = \sum_{i=1}^{2} u_i G_i(q), \quad \min_{u(.)} \int_0^T (u_1^2 + u_2^2)dt,$$

where the cost is defined for a fixed final time $T$ and corresponds to the energy. In this representation, we assume that the vector fields $G_1, G_2$ are orthonormal.

*Remark 3:* For the swimming copepod swimmer an orthonormal frame can be computed as follow. Using the feedback transformation

$$\begin{pmatrix} u_1 \\ u_2 \end{pmatrix} = \begin{pmatrix} \cos\alpha & \sin\alpha \\ -\sin\alpha & \cos\alpha \end{pmatrix} \begin{pmatrix} v_1 \\ v_2 \end{pmatrix}$$

where $\alpha = \arctan\left(\frac{\sin\theta_1}{\sin\theta_2}\right)$, the mechanical cost takes the form

$$\tfrac{1}{3}v_1^2 + \tfrac{1}{6}\,\tfrac{2+\cos^2\theta_2+\cos^2\theta_1}{4-\cos^2\theta_1-\cos^2\theta_2}v_2^2.$$

Introducing $w_1 = \frac{1}{\sqrt{3}}v_1$, $w_2 = \sqrt{\frac{1}{6}\,\frac{2+\cos^2\theta_2+\cos^2\theta_1}{4-\cos^2\theta_1-\cos^2\theta_2}}v_2$ we obtain the metric $w_1^2 + w_2^2$.

The admissible controls are bounded measurable mappings. According to the Pontryagin maximum principle, we introduce the pseudo-Hamiltonian in the normal case

$$H(z, u) = \sum_{i=1}^{2} u_i H_i(z) - \frac{1}{2}\sum_{i=1}^{2} u_i^2,$$

where the $H_i$'s are the Hamiltonian lifts $\langle p, G_i(q)\rangle$. The maximization condition is equivalent to $\frac{\partial H}{\partial u_i} = 0$, $i = 1, 2$. It follows that $u_i = H_i$ and plugging this expression for $u_i$ into $H$ produces the true Hamiltonian in the normal case

$$H_n = \frac{1}{2}\left(H_1^2 + H_2^2\right).$$

In the contact situation, it corresponds to the Heisenberg case while in the Martinet situation, it corresponds to the flat

Martinet case. In both cases it is equivalent to impose that $G_1, G_2$ are orthonormal and that the associated distribution is nilpotent.

*Definition 2:* A normal stroke is a solution of $\overrightarrow{H_n}$ such that $\theta_1$ and $\theta_2$ are periodic with period $T$.

According to the transversality conditions of the maximum principle the dual variables $p_2$ and $p_3$ are such that $p_2$ and $p_3$ are both periodic of period $T$ (to produce a smooth solution).

**Second order optimality condition.** In the normal case, the *first conjugate point* corresponds to the first point where a normal geodesic ceases to be minimizing with respect to the $C^1$-topology on the set of curves and they can be computed using the `HamPath` software [10].

This leads to the following definition.

*Definition 3:* A normal stroke is called $C^1$-optimal on $[0, T]$ if there exists no conjugate point on the interval $]0, T]$.

## III. Numerical computations and analysis in the copepod swimmer

The period $T$ is fixed to $2\pi$ in our simulations. We use the `HamPath` software [10] for:

1) Solving the shooting equations associated with the problem and given by

$$x_0(0) = 0, \qquad x_0(2\pi) = x_f,$$
$$\theta_{1|2}(0) = \theta_{1|2}(2\pi), \qquad p_{2|3}(0) = p_{2|3}(2\pi).$$

2) Showing that the normal stroke is optimal. This is done by testing the nonexistence of conjugate points using the variational equation to compute the Jacobi fields. Recall that according to [7], given a reference curve $(q(t), p(t))$ solution of $\overrightarrow{H_n}$, a time $t_c \in ]0, 2\pi]$ is a conjugate time if there exists a Jacobi field $\delta z = (\delta q, \delta p)$, that is a non-zero solution of the variational equation

$$\dot{\delta z}(t) = \frac{\partial \vec{H}_n}{\partial z}(q(t), p(t))\delta z(t) \tag{7}$$

such that $\delta q(0) = \delta q(t_c) = 0$. We denote $\delta z_i = (\delta q_i, \delta p_i)$, $i = 1, ..., n$, $n$-independent solutions of (7) with initial condition $\delta q(0) = 0$. At time $t_c$ we have the following rank condition

$$\text{rank}\{\delta q_1(t_c), ..., \delta q_n(t_c)\} < n. \tag{8}$$

*1) Commented numerical results:* We present a sequence of numerical simulations for both costs, not taking into account the state constraints. In the two cases we obtain similar results.

- A sequence of three identical normal strokes is represented on Fig.3-4 for the two costs where $x_0(2\pi) = 0.2$. Numerical simulations show the non existence of conjugate points for both cases.
- Fig.5-6-7 illustrate three different strokes illustrating the complexity of the model and are related to the generic classification of periodic planar curves [3].
  Conjugate points are also computed to check the second order optimality conditions. There is no conjugate points on $[0, 2\pi]$ in the case of the simple loop whereas they appear for the limaçon case, the eight case and more complicated cases. *Hence, the only candidates for optimality are the simple loops.*

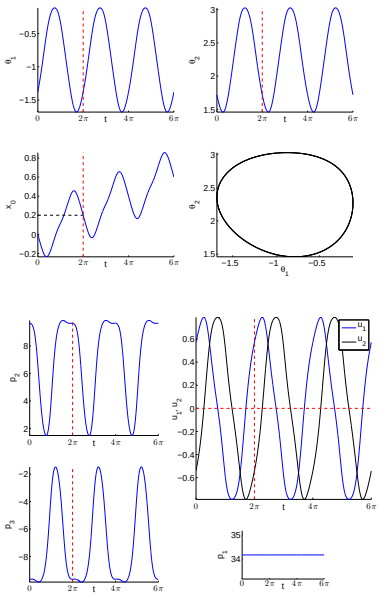

Fig. 3. A sequence of three identical normal strokes for the simplified cost $\int_0^{2\pi}(u_1^2 + u_2^2)\mathrm{d}t$ (state, adjoint and control variables).

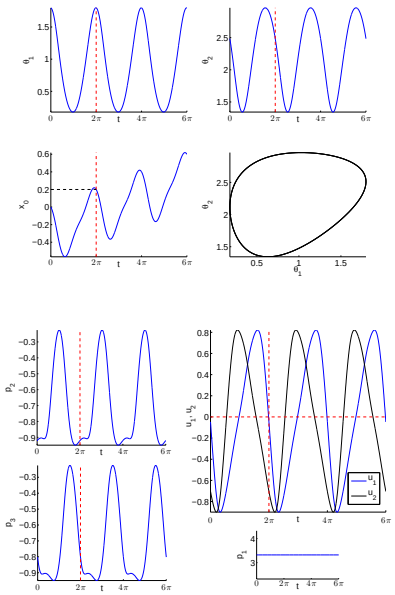

Fig. 4. A sequence of three identical strokes for the mechanical cost (state, adjoint and control variables).

*2) Optimal curves circumscribed in the triangle of constraints:* We use a combination of the `Bocop` and `HamPath` softwares.

`Bocop` software: This software is suitable to take into account constraints on the state variables. Fig.8 gives numerical simulations with this software, describing a creeping normal stroke in accordance with the abnormal

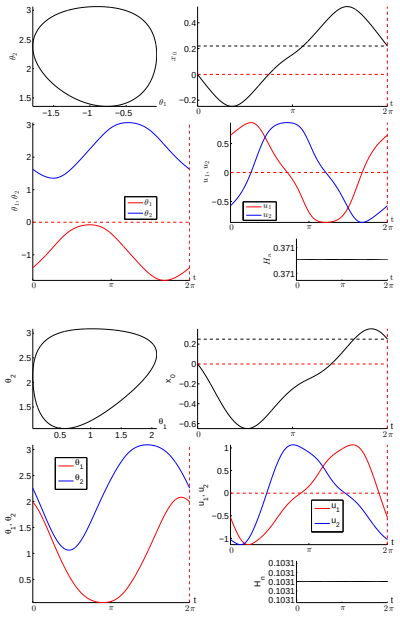

Fig. 5. Normal stroke for the $\int_0^{2\pi}(u_1^2+u_2^2)\mathrm{d}t$ cost (top) and the mechanical cost (bottom): simple loop.

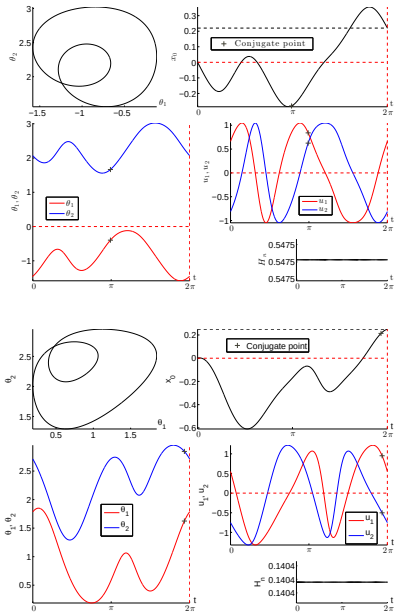

Fig. 6. Normal stroke for the $\int_0^{2\pi}(u_1^2+u_2^2)\mathrm{d}t$ cost (top) and the mechanical cost (bottom): limaçon with inner loop.

triangle policy.

Fig.9 describes a single loop tangent to the boundary which is used to initialize the shooting algorithm of the `HamPath` software.

`HamPath` software: This software cannot be directly applied to compute the optimal solution using the Maximum Principle with state constraints, due to the complexity of the different principles [8].

Fig.10 describes a normal stroke tangent to the boundary.

*3) Comparisons of the geometric efficiency of the strokes:* To compare the different normal and abnormal

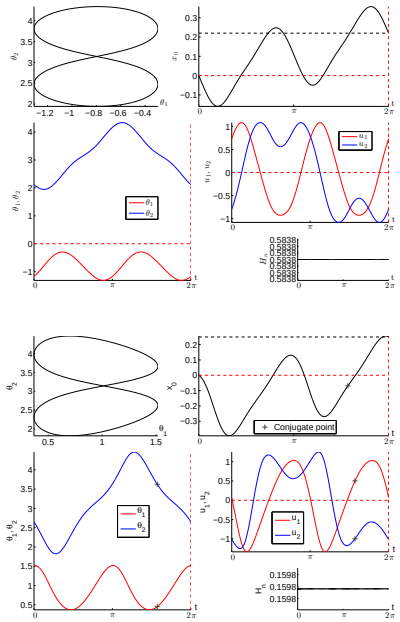

Fig. 7. Normal stroke for the $\int_0^{2\pi}(u_1^2+u_2^2)\mathrm{d}t$ (top) and the mechanical cost (bottom): eight case.

solutions corresponding to different displacements and in relation with the SR-interpretation we represent the ratio $E = x_0/L$ where $L$ is the length of the stroke and $x_0$ is the corresponding displacement (this quantity does not depend upon the parameterization).

For the triangle, a displacement along the vertical or horizontal edge gives $x_0 = \frac{2\sqrt{3}}{3}\operatorname{arctanh}\left(\frac{\sqrt{3}}{3}\right)$ and along the hypotenuse $x_0 = -\sqrt{2}\operatorname{arctanh}\left(\frac{\sqrt{2}}{2}\right)$ and the total displacement is $2.742.10^{-1}$.

The length of a normal stroke $\gamma$ is $L(\gamma) = \int_0^{2\pi}\sqrt{\langle\dot{q},\dot{q}\rangle}\mathrm{d}t$ and easily computed using the energy level $H_n = \frac{1}{2}\langle\dot{q},\dot{q}\rangle = c$ and is $2\pi\sqrt{2c}$. The efficiency curves for the simplified and the mechanical energy are presented in the figures 11-12. The normal strokes corresponding to the maximal efficiency are represented in 11-12. Note that the geometric efficiency $E$ is different from the concept of efficiency of the literature which takes into account the parametrization and the initial shape of the stroke [9].

**Application.** From our analysis we deduce that the (triangle) abnormal stroke is not optimal (for both costs). Indeed, one can choose a normal stroke (inside the triangle) such that the displacement is $\bar{x}_0/2$ with $\bar{x}_0 = 2.742$ and length $< \bar{L}/2$ where $\bar{L}$ =length of the triangle. Applying twice the normal stroke, we obtain the same displacement $\bar{x}_0$ than with the abnormal stroke but with a length $< \bar{L}$.

## IV. Conclusion

In this article we have investigated the copepod swimmer showing:

- from the micro-local point of view various topological strokes (simple loop, eight, limaçon, ...) are obtained confirming the complexity of the model.

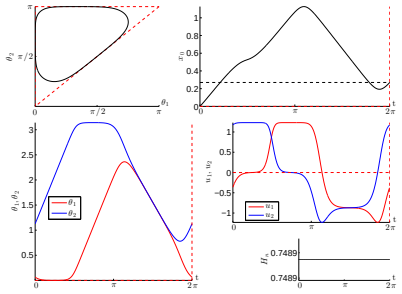

Fig. 8. Creeping normal stroke for the $\int_0^{2\pi}(u_1^2+u_2^2)\mathrm{d}t$ cost obtained by the `Bocop` software.

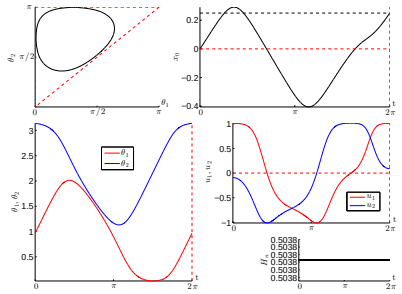

Fig. 9. Tangential normal stroke for the $\int_0^{2\pi}(u_1^2+u_2^2)\mathrm{d}t$ cost obtained by the `Bocop` software.

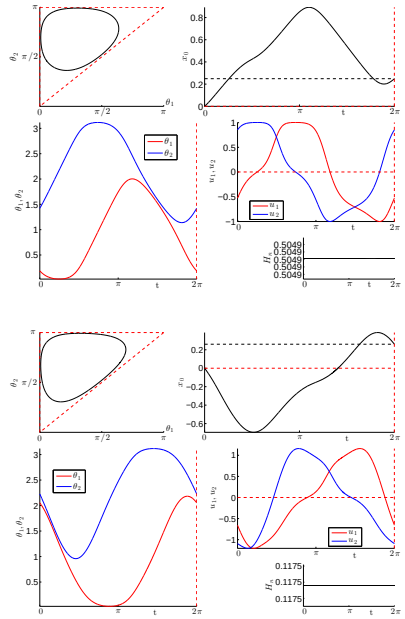

Fig. 10. Normal stroke for the $\int_0^{2\pi}(u_1^2+u_2^2)\mathrm{d}t$ cost (top) and the mechanical cost (bottom) where the constraints are satisfied (simple loop).

- Using second order optimality conditions only simple loops are candidates for optimality.
- The abnormal triangle forming the boundary of the domain is shown to be not optimal, using the computation of the efficiency.

This numerical study open the road to analyze the more complicated Purcell three-link swimmer, see [5] for preliminary results.

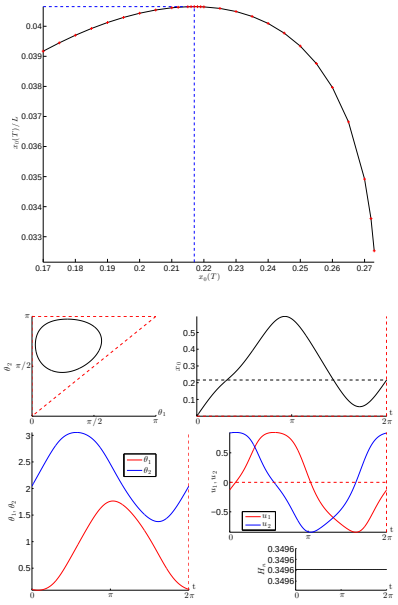

Fig. 11. Efficiency curve for the energy cost (top) and the corresponding minimizing curve (bottom). The efficiency of the abnormal curve is $\mathbf{2.56}e^{-\mathbf{2}}$.

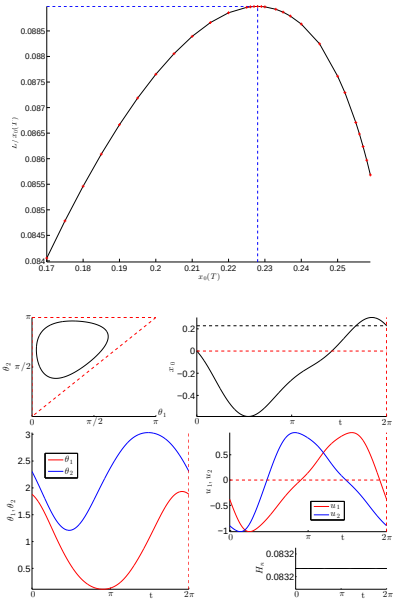

Fig. 12. Efficiency curve for the mechanical cost (top) and the corresponding minimizing curve (bottom). The efficiency of the abnormal curve is $\mathbf{5.56}e^{-\mathbf{2}}$.

## References


[1] Alouges, F., DeSimone, A., Giraldi, L., Zoppello, M.: Self-propulsion of slender microswimmers by curvature control: N-link swimmers. Int. J. Nonlinear Mech. **56** (2013)

[2] Alouges, F., DeSimone, A., Lefebvre, A.: Optimal strokes for low Reynolds number swimmers: an example. J. Nonlinear Sci. **18**, 277–302 (2008)

[3] Berger, M.: La taxonomie des courbes. Pour la science, 297 56–63 (2002)

[4] Becker, L.E., Koehler, S.A., Stone, H.A.: On self-propulsion of micro-machines at low Reynolds number: Purcell's three-link swimmer. J. Fluid Mech. **490**, 15–35 (2003)

[5] Bettiol, P., Bonnard, B., Giraldi, L., Martinon, P., Rouot, J.: The Purcell Three-link swimmer: some geometric and numerical aspects related to periodic optimal controls. Rad. Ser. Comp. App. **18**, Variational Methods, Ed. by M. Bergounioux et al. (2016)

[6] Bonnans, F., Giorgi, D., Maindrault, S., Martinon, P., Grélard, V.: Bocop - A collection of examples, Inria Research Report, Project-Team Commands. **8053** (2014)

[7] Bonnard, B., Chyba, M.: Singular trajectories and their role in control theory. Mathématiques & Applications **40**, Springer-Verlag, Berlin (2003)

[8] Bonnard, B., Faubourg, L., Trélat, E.: Mécanique céleste et contrôle des véhicules spatiaux. Mathématiques & Applications **51**, Springer-Verlag Berlin (2006)

[9] Chambrion, T., Giraldi, L., Munnier, A.: Optimal strokes for driftless swimmers: A general geometric approach. *Submitted* (2014)

[10] Cots, O.: Contrôle optimal géométrique: méthodes homotopiques et applications. PhD thesis, Université de Bourgogne (2012)

[11] Giraldi J., Martinon, P., Zoppello, M.: Optimal design of the three-link Purcell swimmer. Phys. Rev. E **91** (2015)

[12] Gray, J., Hancock, G. J.: The propulsion of sea-urchin spermatozoa. J. Exp. Biol. **32**, 802–814 (1955)

[13] Hakavuori, E., Le Donne, E.: Non-minimality of corners in sub-Riemannian geometry. Preprint (2015)

[14] Lauga, E., Powers, T.R.: The hydrodynamics of swimming microorganisms. Rep. Progr. Phys. **72**, 9 (2009)

[15] Passov, E., Or, Y.: Supplementary notes to: Dynamics of Purcell's three-link microswimmer with a passive elastic tail. EPJ E **35**, 1–9 (2012)

[16] Lenz, P. H., Takagi, D., Hartline,D. K.: Choreographed swimming of copepod nauplii. J. R. Soc. Interface 12, 20150776 (2015)

[17] Purcell, E.M.: Life at low Reynolds number. Am. J. Phys. **45**, 3–11 (1977)

[18] Takagi, D.: Swimming with stiff legs at low Reynolds number. Phys. Rev. E 92. (2015)

[19] Tam, D., Hosoi, A.E.: Optimal Stroke Patterns for Purcell Three-Link Swimmer. Phys. Rev. Lett. **98** (2007)

[20] Taylor, G.I.: Analysis of the swimming of microscopic organisms. Proc. Roy. Soc. London. Ser. A. **209**, 447–461 (1951)

[21] Zhitomirskiĭ, M.: Typical singularities of differential 1-forms and Pfaffian equations. American Mathematical Society, Providence, RI. **113** (1992)